Published by Elsevier Inc.

ISSN 0735-1097/04/$30.00
doi:10.1016/j.jacc.2004.04.042

PRECLINICAL RESEARCH

Treatment of Acute Myocardial Infarction by Hepatocyte Growth Factor Gene Transfer

The First Demonstration of Myocardial Transfer of a "Functional" Gene Using Ultrasonic Microbubble Destruction

Isao Kondo, MD, PHD, Koji Ohmori, MD, PHD, Akira Oshita, MD, PHD, Hiroto Takeuchi, MD, PHD, Sachiko Fuke, DVM, MCS, Kaori Shinomiya, MD, PHD, Takahisa Noma, MD, PHD, Tsunetatsu Namba, MD, PHD, Masakazu Kohno, MD, PHD

Kagawa, Japan

OBJECTIVES We examined whether ultrasonic microbubble destruction (US/MB) enables therapeutic myocardial gene transfer of hepatocyte growth factor (HGF) for acute myocardial infarction (MI).

BACKGROUND Hepatocyte growth factor gene transfer provides cardioprotective effects in MI, which requires direct intramyocardial injection or special vectors. Although US/MB was used in myocardial gene transfer, its feasibility in transfer of a therapeutic gene with non-viral vector remains unknown.

METHODS In a rat model of acute MI, naked plasmid (pVax1) encoding human HGF (1,500 μg) was infused into the left ventricular (LV) chamber during US/MB (HGF-US/MB) or insonation only (HGF-US) or alone (HGF-alone), while control MI rats received empty pVax1 during US/MB (pVax1-US/MB). For US/MB, transthoracic intermittent insonation with a diagnostic transducer (1.3 MHz) was performed for 2 min at a peak negative pressure of −2,160 kPa during intravenous 20% Optison.

RESULTS Baseline risk area was comparable among the groups. Immunohistology seven days after treatment revealed significant myocardial expression of HGF protein only in HGF-US/MB. At three weeks, LV weight in HGF-US/MB (0.89 ± 0.03 g) was significantly lower than those in HGF-alone (1.09 ± 0.08 g), HGF-US (1.04 ± 0.07 g), and pVax1-US/MB (1.04 ± 0.05 g). Moreover, scar size was significantly smaller (16 ± 6% vs. 39 ± 5%, 41 ± 6%, and 40 ± 4% of total myocardial circumferential length, respectively), while capillary density (49 ± 8 vs. 34 ± 5, 37 ± 6, and 36 ± 4 capillaries/high-power field, respectively) and arterial density (37 ± 7 vs. 15 ± 9, 18 ± 4, and 14 ± 11 arterioles/high-power field, respectively) in the risk area were higher in HGF-US/MB than the other groups.

CONCLUSIONS Ultrasound-mediated microbubble destruction may enable myocardial HGF gene transfer with systemic administration of naked plasmid, which enhances angiogenesis, limits infarction size, and prevents LV remodeling after MI. (J Am Coll Cardiol 2004;44:644–53)

Acute myocardial infarction (MI) leads to left ventricular (LV) remodeling, including expansion or aneurysm formation due to cardiomyocyte death in infarcted regions and LV dilation associated with hypertrophy and fibrosis of non-infarcted regions (1).

Hepatocyte growth factor (HGF) exhibits pleiotropic effects on various cells (2). Previous studies have demonstrated that c-Met/HGF receptor is expressed also in cardiomyocytes and that HGF prevents myocyte death due to oxidative stress (3) and cardiomyocyte apoptosis during reperfusion (4). Hepatocyte growth factor gene transfection before myocardial ischemia attenuates reperfusion injury (5), while the transfection by direct intramyocardial injection immediately after coronary ligation induces angiogenesis in infarcted myocardium (6). Thus, HGF gene therapy may be applicable to the treatment of MI.

Adenoviral vectors were used in gene delivery (7,8) because the transfection efficiency is high. However, unfavorable immune responses of the host (9) have promoted the development of non-viral gene delivery techniques. Although a direct injection of naked plasmid DNA may be a solution (10–14), the direct injection into the myocardium requires surgical procedures (13) or catheter-based endomyocardial approaches (14).

Recently, ultrasound-induced microbubble destruction (US/MB) has been proposed as a new technique for site-specific gene delivery (15–22). Microbubbles (MBs) currently used as ultrasound (US) contrast agents can lower the energy threshold of US for cavitation, which transiently perforates the cell membrane (18,19) or disrupts the capillary wall to allow delivery of bioactive agents into cells (18) or interstitial space (15,16). In this regard, US/MB has been

From the Second Department of Internal Medicine, Kagawa University School of Medicine, Kagawa, Japan.

Manuscript received December 25, 2002; revised manuscript received April 12, 2004, accepted April 20, 2004.

Abbreviations and Acronyms

HGF = hepatocyte growth factor
LV = left ventricle/ventricular
MB = microbubble
MCE = myocardial contrast echocardiography
MI = myocardial infarction
US = ultrasound
US/MB = ultrasound-mediated microbubble destruction

shown to enhance the adenovirus-mediated myocardial transfection of a reporter gene (17,22) with transthoracic insonation. However, the transfer of a functional gene to the myocardium with a naked plasmid in combination with US/MB has not been demonstrated. Therefore, we tested the hypothesis that myocardial-targeted disruption of MBs by transthoracic insonation may enable myocardial gene transfer of HGF encoded in a naked plasmid that is infused into the circulating blood pool to ameliorate the pathology in acute MI in rats.

METHODS

Naked HGF plasmid. We used a naked HGF plasmid (AnGes MG Inc., Tokyo, Japan), in which human HGF complementary DNA (2.2 kb) was inserted into a eucaryotic expression plasmid pVax1 (Invitrogen, Tokyo, Japan) that utilizes the cytomegalovirus promoter/enhancer (11). The vector pVax1 that did not contain HGF complementary DNA was used as a control plasmid.

Animal preparation. The study protocol was approved by the animal research committee of our institution. A total of 68 male Sprague-Dawley rats (250 to 300 g) were anesthetized with an intraperitoneal injection of sodium pentobarbital (65 mg/kg). A polyethylene catheter (PE10) was advanced into LV through the right external carotid artery for plasmid injection. The left femoral artery and vein were cannulated for blood pressure and heart rate measurements and for MB infusion, respectively. The animals were ventilated with room air using a respirator SN-480-7 (Shinano, Tokyo, Japan). A left lateral thoracotomy was performed at the fourth intercostal space. The left coronary artery was completely ligated 2 mm distal to its origin from the aorta using a 4.0 silk ligature. After the removal of air in the chest, the incision was closed by sutures. The subsequent procedures in our protocol are shown in Figure 1.

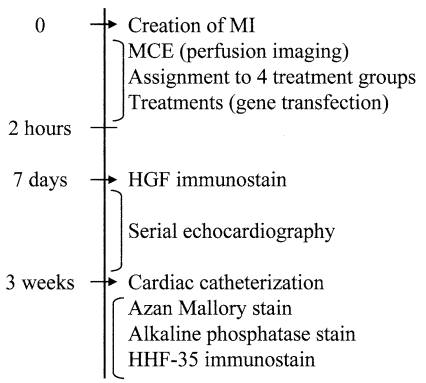

Figure 1. Protocol of this study. Various treatments following myocardial contrast echocardiography (MCE) were performed within 2 h after the onset of myocardial infarction (MI). Half of the rats in each group were killed on day 7 for myocardial hepatocyte growth factor (HGF) immunostain. The rest of the rats underwent serial echocardiography until week 3, when they were subjected to cardiac catheterization and were killed for histopathologic assessments.

Determination of myocardial risk area during coronary occlusion. Myocardial contrast echocardiography (MCE) was performed using a broadband (5 to 12 MHz) transducer S12 of SONOS 5500 (Philips Medical Systems, Andover, Massachusetts) and 10% Optison (Tyco Health Care/Mallinckrodt Inc., St. Louis, Missouri), which was intravenously infused at 0.2 ml/min by a syringe pump up to a total maximal dose of 0.6 ml. Short-axis images of the LV at the mid-papillary muscle level were obtained in the fundamental mode, which provided quantitative myocardial opacification in rats (23), with a mechanical index of 1.1 triggering at every 4th end-systole (Fig. 2A), which were recorded on MO disks. The size of the risk area was expressed as a percentage of the myocardial area exhibiting an opacification defect in the total LV myocardial area.

HGF gene transfer with ultrasonic microbubble destruction. After MCE, the rats were assorted into four treatment groups as follows: HGF plasmid administration in combination with US/MB (HGF-US/MB) (n = 16), control vector administration in combination with US/MB (pVax1-US/MB) (n = 13), HGF plasmid administration with ultrasound alone (HGF-US) (n = 12), and HGF plasmid infusion only (HGF-alone) (n = 15). The treatments were performed within 2 h after coronary ligation. A total of 20% Optison was infused via the femoral vein at 0.2 ml/min for 5 min. One min after the initiation of MB infusion, HGF plasmid (1,500 μg) or control pVax1 plasmid (1,500 μg) was infused into the blood pool via LV catheter for 1.5 min at 1 ml/min. Simultaneously, with the plasmid infusion, insonation was started with an S3 transducer of SONOS 5500 (Philips Medical Systems) operating in ultraharmonic mode (transmit 1.3 MHz/receive 3.6 MHz), which was continued for 4 min. Ultrasound of a peak negative pressure of −2,160 kPa was transmitted as a burst of three frames at 28 Hz triggered at every 8th end-systole with the focus in the center of LV cavity (Fig. 2B). Each burst eliminated all MBs visible in the myocardium, and pulsing-interval of eight cardiac cycles allowed complete replenishment of MBs before the next burst (17). In the HGF-US, insonation was performed in the same manner for 4 min during intravenous infusion of saline instead of 20% Optison. No insonation was performed in the HGF-alone group during intravenous infusion of saline for Optison. Thus, all rats excepting those in the HGF-alone group were exposed to the same insonation, and all rats received 2.5 ml of fluid in 5 min during the treatments. To prevent congestive heart failure due to volume overload,

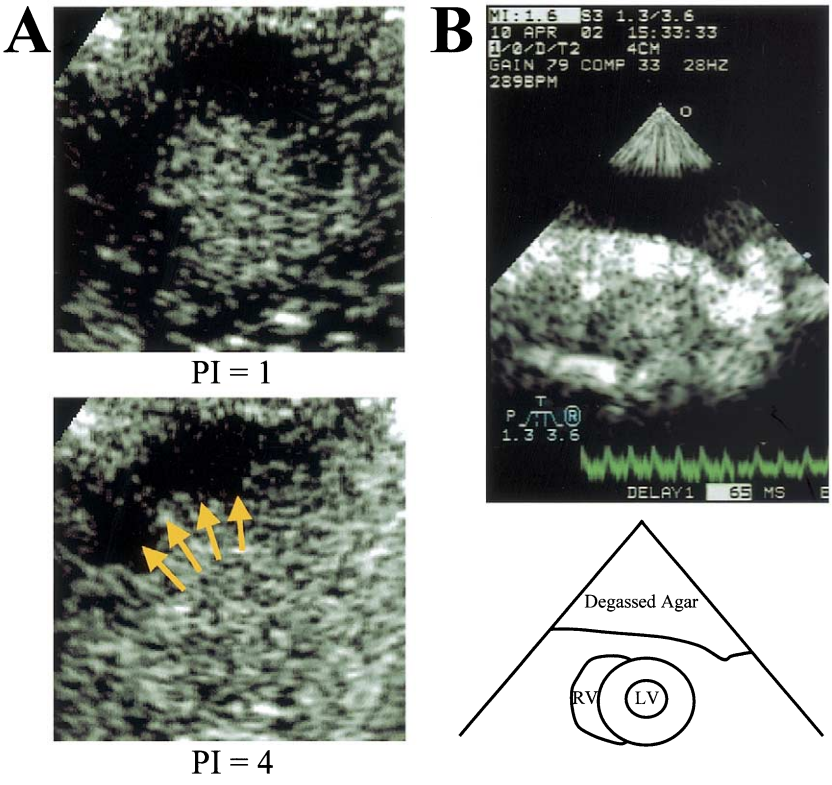

Figure 2. (A) Representative recordings of intermittent short-axis images during myocardial contrast echocardiography after coronary occlusion at pulsing interval (PI) of every cardiac cycle (PI = 1) and of every 4th end systole (PI = 4). **Arrows** denote the risk area. **(B)** The first frame of the three-frame burst during hepatocyte growth factor gene transfer with ultrasonic microbubble destruction is shown **(top)** with an illustration **(bottom)**.

furosemide (0.4 mg/kg) was intramuscularly injected before the treatments in all rats.

Assessment of LV remodeling and functional reserve. Transthoracic echocardiographic studies were performed with the S12 transducer every week after the treatments to evaluate serial changes in LV dimensions and wall thickness. After the final echocardiographic studies at three weeks after the treatments, LV pressure was measured with an ultraminiature transducer SPR-671 (Millar Instruments, Inc., Houston, Texas) via the right common carotid artery. The peak positive and negative values of the first derivative of LV pressure (Max-dP/dt, Min-dP/dt) and developed pressure as the difference in peak systolic and end-diastolic pressures before and during isoproterenol (10^{-7} mol/l) infusion (0.2 ml over 1 min) were derived. After the hemodynamic studies, adequate anesthesia was achieved, and the heart was removed. After LV weight measurement, the LV was sliced at the short axis in 3 mm thickness. A part of the LV was frozen at −80°C, and the rest of the LV was immersed in a cold 4% paraformaldehyde solution for 24 h for Azan-Mallory staining and immunohistochemistry.

Histopathologic analyses. One-half of the rats in each group were killed at seven days after treatment for determination of HGF expression by immunohistology. Immunostaining of HGF was performed on paraffin-embedded sections by using primary antibodies to human HGF (Dako, Carpinteria, California) with a commercial kit (Nitirei, Tokyo, Japan). Endogenous peroxidase was inactivated by treatment with 3% H_2O_2 in 0.01 M phosphate-buffered saline (pH 7.4) for 15 min. Any non-specific immunoreactivity was inhibited by pre-incubation with 1% bovine serum albumin, phosphate-buffered saline, and 0.1% Tween 20. Antibody against HGF was placed on the slides and was incubated for 24 h. The slides were washed and stained with 3,3′-diaminobenzidine (Nitirei, Tokyo, Japan). The magnitude of HGF expression was semi-quantitated by a scoring system: 0 = absent; 1 = patchy; 2 = homogeneous stain. Reproducibility of the score was assessed in randomly selected 10 slides each of which yielded two scores, one for the marginal viable segment and the other for the remote control region. The Kappa statistics (24) indicated that the intra- and inter-observer agreements were good (kappa = 0.68 and 0.63, respectively).

The remaining rats that underwent serial echocardiographic examinations and cardiac catheterization were subjected to histopathology at three weeks after MI. Azan-Mallory stain was used to determine the scar corresponding to infarction, which was quantitated as a percentage of the scar length to the total circumferential length of the LV myocardial mid-wall at the mid-ventricular level. Angiogenesis was assessed using endothelial alkaline phosphatase staining (25). Arteriogenesis was assessed with immunohis-

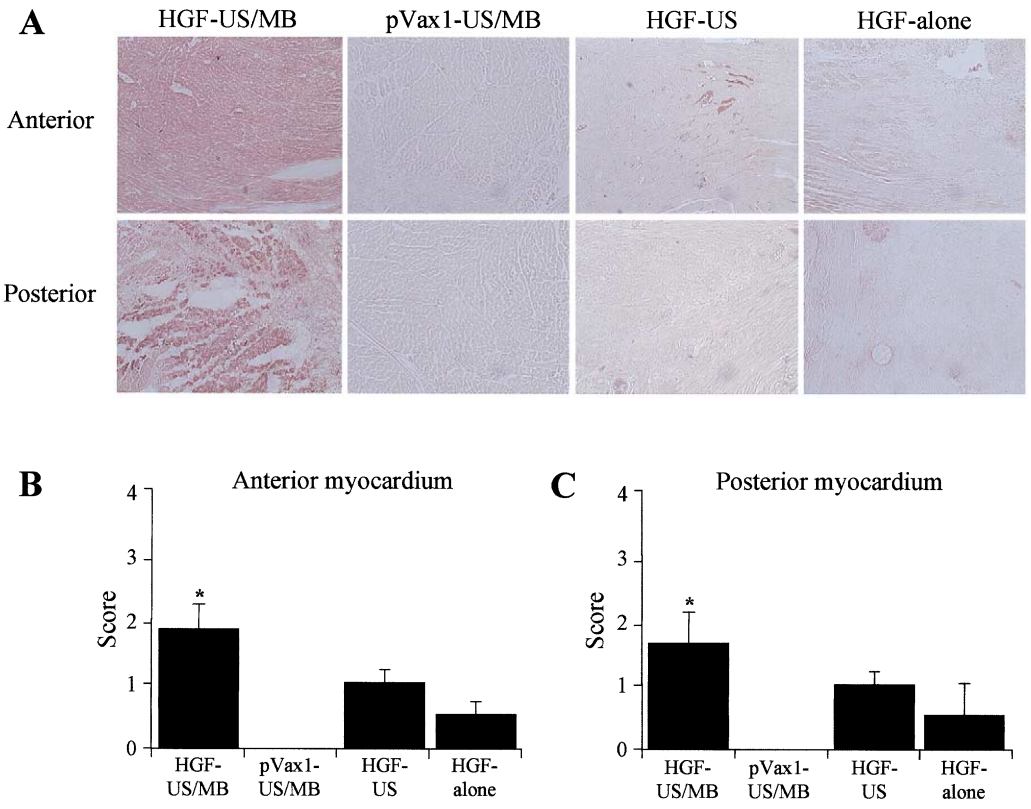

Figure 3. Immunohistology for hepatocyte growth factor (HGF) at ×400 magnification. **(A)** Sections obtained from the anterior region adjacent to the scar **(top)** and that obtained from the remote control posterior region **(bottom)** were shown. Naked HGF plasmid infusion with ultrasound-mediated microbubble destruction (US/MB) (HGF-US/MB) exhibited positive staining of HGF in both regions. Hepatocyte growth factor stain was negative in control plasmid infusion with US/MB (pVax1-US/MB) and was limited to perivascular regions in naked plasmid HGF infusion during insonation (HGF-US) and naked HGF plasmid infusion without US/MB (HGF-alone) in both regions. **Bar graphs** compare the score of the magnitude of HGF expression among the groups for the regions adjacent to the scar **(B)** and for the remote non-infarcted regions **(C)**. *$p < 0.05$ versus pVax1-US/MB, HGF-US, and HGF-alone.

tochemical staining with HHF-35 (Dako), a murine monoclonal antibody against endogenous α-smooth muscle actin (11,25), which stained primarily medium and large arteries (25). Capillary density and small arterial density (diameter <100 μm) were quantitated by counting the vessel number per high-power field.

Hepatocyte growth factor expression and angiogenesis were evaluated in the viable regions adjacent to the scar and in the remote control areas. At least three portions per region were analyzed for each heart. The observers were blinded to the identification of the specimens.

Statistical analysis. All data are expressed as mean ± SD. Differences in mortality rates among the treatment groups were assessed by chi-square test, while those at specific stages between groups were assessed by one-way analysis of variance (ANOVA) with Bonferroni's correction. One-way repeated measures of ANOVA with Bonferroni's correction were used in testing serial changes. Changes in the parameters by isoproterenol were assessed by paired Student *t* test. Differences were considered significant at $p < 0.05$ after the correction for comparisons between HGF-US/MB versus each of the other three groups.

RESULTS

Fifty-six of 68 rats survived after the onset of MI and MCE and were subjected to the various treatments. Although seven rats died during or immediately after the treatments, no rats died subsequently until the final evaluation at three weeks, except 24 rats that were sacrificed on day 7 for HGF immunostaining. There was no difference in the mortality rate in the four groups by day 7: 12.5% (2 of 16) in HGF-US/MB, 8% (1 of 13) in pVax1-US/MB, 8% (1 of 12) in HGF-US, and 20% (3 of 15) in HGF-alone. Moreover, no significant difference was noted between the rats that received HGF plasmid (6 of 43 = 14.0%) and those that did not (1 of 12 = 8.3%). The size of the risk area of the survivors was comparable among the four groups: 45 ± 5% in HGF-US/MB, 47 ± 4% in pVax1-US/MB, 46 ± 7% in HGF-US, and 47 ± 6% in HGF-alone.

HGF gene transfection by ultrasound microbubble destruction. Homogeneous HGF expression in the marginal regions of the viable area was observed only in HGF-US/MB, while no expression of HGF was observed in pVax1-US/MB, and a patchy perivascular expression was observed in HGF-US group and in HGF-alone group

Table 1. Changes in LV Geometry

	Baseline	1 Week	2 Weeks	3 Weeks
LV end-diastolic diameter (mm)				
HGF-US/MB	7.46 ± 0.35	7.94 ± 0.55*†‡	8.17 ± 0.59*‡§	8.26 ± 0.60*
pVax1-US/MB	7.38 ± 0.21	8.22 ± 0.18	8.90 ± 0.23§	9.22 ± 0.30§
HGF-US	7.40 ± 0.20	8.26 ± 0.21	8.94 ± 0.21§	9.32 ± 0.28§
HGF-alone	7.43 ± 0.40	8.55 ± 0.30	9.12 ± 0.55§	9.68 ± 0.74§
LV end-systolic diameter (mm)				
HGF-US/MB	6.69 ± 0.55	6.74 ± 0.53*†‡	6.76 ± 0.45*†‡	6.66 ± 0.47*†‡
pVax1-US/MB	6.35 ± 0.28	7.22 ± 0.19§	7.92 ± 0.35§	8.17 ± 0.29§
HGF-US	6.44 ± 0.30	7.31 ± 0.20§	7.98 ± 0.35§	8.22 ± 0.31§
HGF-alone	6.47 ± 0.33	7.57 ± 0.68§	8.12 ± 0.51§	8.62 ± 0.74§
IVS thickness (mm)				
HGF-US/MB	1.58 ± 0.05	1.44 ± 0.12*†‡§	1.27 ± 0.16*†‡§	1.27 ± 0.15*†‡§
pVax1-US/MB	1.57 ± 0.06	1.26 ± 0.08§	1.09 ± 0.10§	1.08 ± 0.09§
HGF-US	1.58 ± 0.05	1.25 ± 0.07§	1.08 ± 0.09§	1.08 ± 0.09§
HGF-alone	1.58 ± 0.05	1.26 ± 0.07§	1.08 ± 0.11§	1.07 ± 0.06§
LV posterior wall thickness (mm)				
HGF-US/MB	1.61 ± 0.06	1.60 ± 0.07	1.59 ± 0.06	1.60 ± 0.08
pVax1-US/MB	1.59 ± 0.09	1.61 ± 0.06	1.59 ± 0.05	1.60 ± 0.08
HGF-US	1.60 ± 0.08	1.60 ± 0.08	1.59 ± 0.08	1.59 ± 0.08
HGF-alone	1.59 ± 0.08	1.58 ± 0.07	1.58 ± 0.08	1.58 ± 0.10
Fractional shortening (%)				
HGF-US/MB	10.4 ± 5.0	15.2 ± 7.6	17.1 ± 6.4	19.1 ± 6.9§
pVax1-US/MB	12.8 ± 4.2	12.2 ± 2.3	11.1 ± 1.7	11.4 ± 2.5
HGF-US	12.7 ± 3.9	12.1 ± 2.8	10.9 ± 2.0	10.9 ± 2.1
HGF-alone	12.9 ± 4.3	11.6 ± 5.3	11.0 ± 2.1	11.0 ± 2.5
LV mass (g)				
HGF-US/MB	0.81 ± 0.09	0.82 ± 0.09	0.82 ± 0.14*†‡	0.83 ± 0.11*†‡
pVax1-US/MB	0.80 ± 0.05	0.81 ± 0.06	0.85 ± 0.06§	0.92 ± 0.07§
HGF-US	0.81 ± 006	0.82 ± 0.07	0.85 ± 0.05§	0.93 ± 0.08§
HGF-alone	0.81 ± 0.08	0.88 ± 0.04§	0.89 ± 0.13§	0.97 ± 0.21§

*$p < 0.05$ versus pVax1-US/MB; †$p < 0.05$ versus HGF-alone; ‡$p < 0.05$ versus HGF-US; §$p < 0.05$ versus baseline.
HGF-alone = naked HGF plasmid infusion without US/MB (n = 6); HGF-US = naked HGF plasmid infusion with ultrasound only (n = 6); HGF-US/MB = naked HGF plasmid infusion with US/MB (n = 7); IVS = intraventricular septum; LV = left ventricular; pVax1-US/MB = control plasmid infusion with US/MB (n = 6); US/MB = ultrasound-mediated microbubble destruction.

(Fig. 3A, top). The patterns of HGF expression were similar in the remote control areas (Fig. 3A, bottom). The score for HGF expression was significantly higher in HGF-US/MB than in the other groups (all, $p < 0.05$) both for the marginal regions of viable area (Fig. 3B) and remote control area (Fig. 3C).

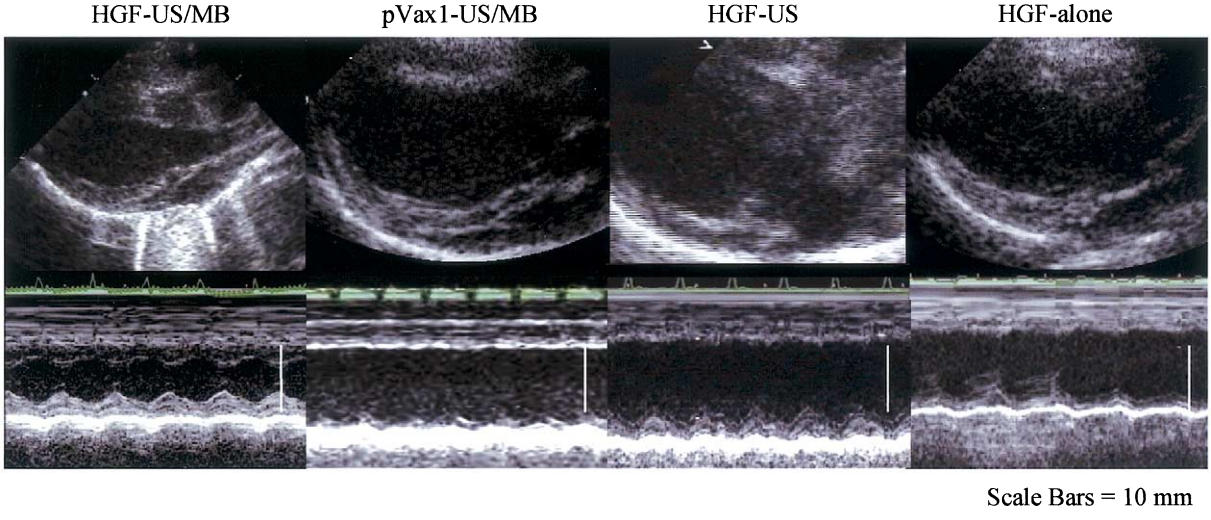

Figure 4. Representative recordings of left ventricular (LV) two-dimensional **(top)** and M-mode **(bottom)** echocardiography at three weeks after the treatments. Left ventricular remodeling was almost completely inhibited in a rat form naked plasmid hepatocyte growth factor (HGF) infusion with ultrasound-mediated microbubble destruction (US/MB) (HGF-US/MB) group, while the intraventricular septum was thinned and LV chamber was dilated in the other groups. Other abbreviations as in Figure 3.

Table 2. Hemodynamic Responses to Isoproterenol Infusion

	HGF-US/MB	pVax1-US/MB	HGF-US	HGF-alone
Systolic pressure (mm Hg)				
Baseline	127 ± 16	115 ± 17	120 ± 11	119 ± 15
Isoproterenol	146 ± 12†§	117 ± 16	126 ± 18	128 ± 22
Developed pressure (mm Hg)				
Baseline	120 ± 16*†‡	100 ± 14	106 ± 12	101 ± 16
Isoproterenol	142 ± 12*†‡§	99 ± 15	111 ± 18	109 ± 27
Heart rate (beats/min)				
Baseline	385 ± 16	388 ± 17	386 ± 14	391 ± 17
Isoproterenol	410 ± 17§	411 ± 9§	418 ± 16§	415 ± 13§
Max-dP/dt (mm Hg/s)				
Baseline	7,699 ± 944*†‡	4,958 ± 745	5,021 ± 680	4,537 ± 900
Isoproterenol	11,943 ± 2,839*†‡§	7,120 ± 889	6,904 ± 902	5,567 ± 1,499
Min-dP/dt (mm Hg/s)				
Baseline	5,113 ± 626*†‡	3,715 ± 701	4,012 ± 401	3,858 ± 353
Isoproterenol	5,914 ± 1,084*†‡	3,812 ± 311	3,942 ± 561	3,551 ± 539

*$p < 0.05$ versus pVax1-US/MB; †$p < 0.05$ versus HGF-alone; ‡$p < 0.05$ versus HGF-US; §$p < 0.05$ versus baseline.
Max-dP/dt = maximum first derivative of left ventricular pressure; Min-dP/dt = minimum first derivative of left ventricular pressure. Other abbreviations and number of rats for each group as in Table 1.

Serial changes in LV geometry. Baseline echocardiographic variables for LV geometry and function were similar among the groups (Table 1). Progressive increases in LV dimensions and LV mass were observed, and fractional shortening failed to improve in the pVax1-US/MB, HGF-US, and HGF-alone groups. However, in the HGF-US/MB, LV end-systolic dimension remained unchanged with a slight increase in end-diastolic dimension, which resulted in unchanged LV mass and improved fractional shortening (Table 1). Thus, at week 3, substantial improvements of LV geometry and function were achieved only in HGF-US/MB as shown in Figure 4, while intraventircular septum was thinned and LV chamber was dilated in the other groups. Left ventricular tissue weight was significantly lower in HGF-US/MB (0.89 ± 0.03 g) than in pVax1-US/MB (1.04 ± 0.05 g), HGF-US (1.04 ± 0.07 g), and HGF-alone (1.09 ± 0.08 g) (all, $p < 0.05$) at week 3. Thus, LV remodeling after MI was successfully prevented only in HGF-US/MB.

Reserve for inotropic stimulation. The baseline (pre-isoproterenol) heart rate and systolic blood pressure at week 3 were similar among the four groups (Table 2). Developed pressure was significantly higher in HGF-US/MB than that in the other groups due to lower LV end-diastolic pressure. The max-dP/dt and min-dP/dt at baseline were greater in HGF-US/MB than those in the other three groups. Although all values increased in response to isoproterenol in HGF-US/MB, only heart rate responded in the other groups (Table 2). Thus, the reserve for inotropic stimulation was preserved only in HGF-US/MB group.

Extent of scar formation. A large scar in the anterior wall was observed on Azan-Mallory-stained sections in a rat from the pVax1-US/MB group (Fig. 5B) and in rats from HGF-US (Fig. 5C) and from HGF-alone (Fig. 5D). In contrast, the scar was much smaller in a rat of HGF-US/MB (Fig. 5A). Thus, scar size was significantly smaller in HGF-US/MB (16 ± 6% of total myocardial mid-wall length) than in pVax1-US/MB (39 ± 5%), HGF-US (41 ± 6%), and HGF-alone (40 ± 4%) (all, $p < 0.05$).

Capillary and artery density. Increase in capillaries in the myocardium adjacent to the infarcted area was observed in a rat from HGF-US/MB as compared with those from the other groups (Fig. 6A, top). Such a difference was not observed in the non-infarcted remote regions (Fig. 6A, bottom). The capillary density in the region adjacent to the infarction was 1.5-fold higher in HGF-US/MB than that in the other groups (all, $p < 0.05$) (Fig. 6B), although the density in non-infarcted regions was comparable among the four groups (Fig. 6C).

A significant increase in arterial count was noted in the region adjacent to the infarcted region in a rat from HGF-US/MB group, compared with that in rats in the

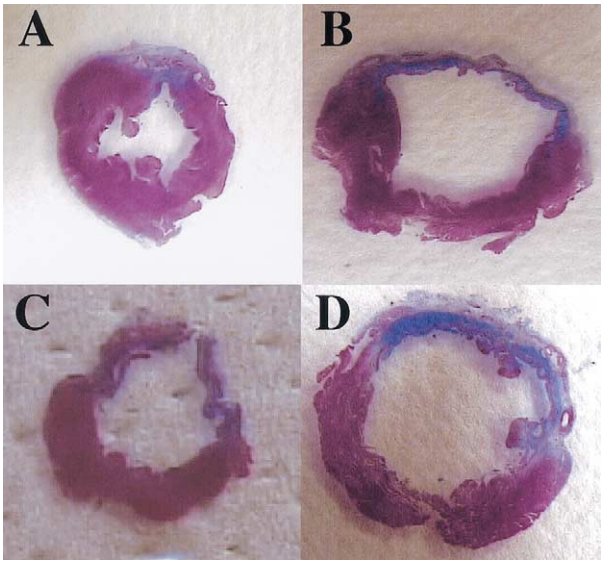

Figure 5. Azan-Mallory stain (×100 magnification). Scar corresponding to the infarction was small in a rat from HGF-US/MB **(A)** compared with those from pVax1-US/MB **(B)**, HGF-US **(C)**, and from HGF-alone **(D)**. Abbreviations as in Figure 3.

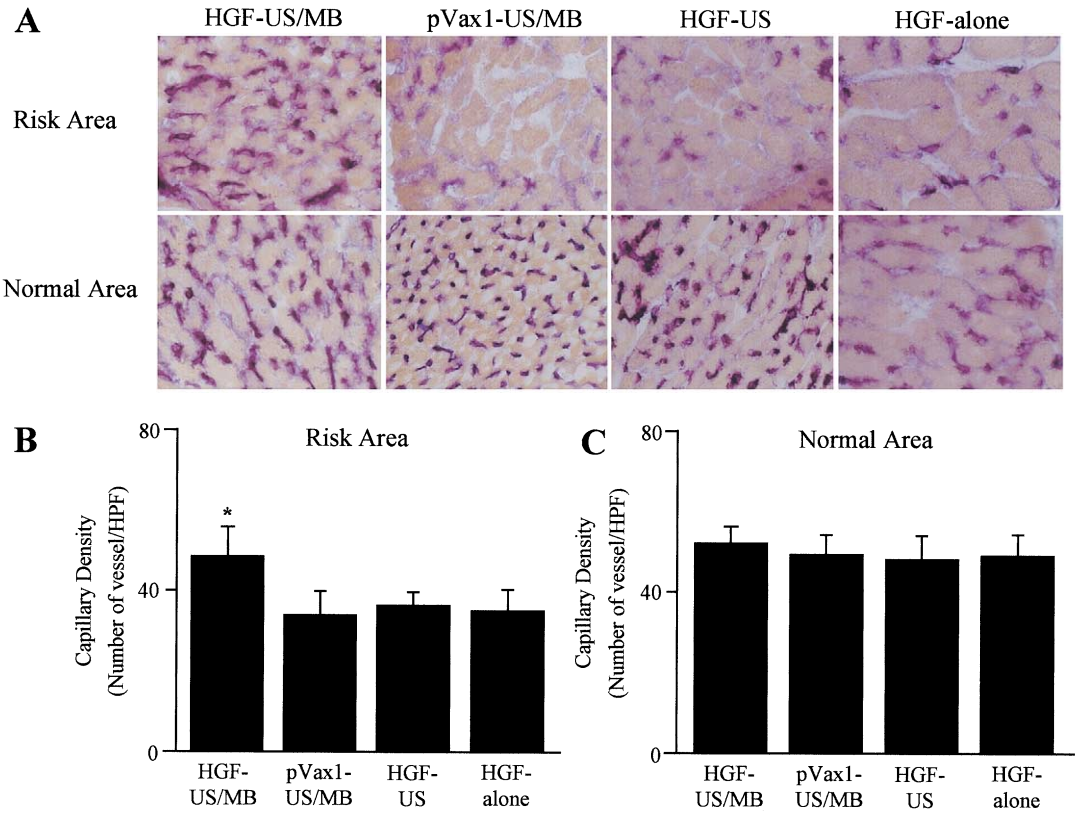

Figure 6. Endothelial alkaline phosphatase stain (×400 magnification). **(A)** In the regions adjacent to the scar, capillary density was significantly higher in a rat from HGF-US/MB than those from other groups **(top)**. No significant differences were noted among the groups in the capillary density in the remote non-infarcted regions **(bottom)**. **Bar graphs** compare the vessel count per high-power field (HPF) among the groups for the regions adjacent to the scar **(B)** and for the remote non-infarcted regions **(C)**. *$p < 0.05$ versus pVax1-US/MB, HGF-US, and HGF-alone. Abbreviations as in Figure 3.

other groups (Fig. 7A, top). Such a difference did not exist in the non-infarcted remote regions (Fig. 7A, bottom). The number of small arteries was threefold higher in the region adjacent to the infarcted area in HGF-US/MB group than that in the other three groups (Fig. 7B) although that in the non-infarcted regions was comparable among the four groups (Fig. 7C). Thus, angiogenesis and arteriogenesis were enhanced in the border zone adjacent to the infarction only in the HGF-US/MB group.

DISCUSSION

This report describes the first successful therapeutic gene delivery to the heart by means of US/MB. The naked plasmid encoding HGF that was infused into the blood pool via the LV chamber was successfully delivered to the myocardium by insonation during intravenous MB infusion. Hepatocyte growth factor gene delivery with this method in the acute phase of experimental MI successfully prevented subsequent scar formation and LV remodeling.

HGF gene transfer with ultrasonic microbubble destruction. Intravital microscopic observations have demonstrated that US disrupts MBs in capillaries, which results in capillary rupture (15,16). In this way, intravenously injected polymer microspheres could be driven as much as 200 μm into the parenchyma (15), which provided the basis for US/MB-mediated microinjection of bioactive agents into tissues through the barrier of vessel wall. In this regard, several investigators have demonstrated that US/MB enables delivery of genes (17–22) to specific tissues, including the myocardium (17,22). Thus, US/MB has been shown to enhance the transfer of endothelial nitric oxide synthase gene using a naked plasmid to the swine coronary artery in vitro (21) and the ex vivo transfection of anti-oncogene p-53 plasmid to the rat carotid artery (20). More recently, US/MB has been used to enhance the delivery of HGF into the skeletal muscle by direct intramuscular injection of a naked plasmid into the rat hind limbs (19). This technique was applied to the heart, and the successful cardiac delivery of a reporter gene expressing β-galactosidase was achieved by using an adenovirus vector loaded on MBs (17). However, for the therapeutic use in patients, innovations in less invasive non-viral plasmid DNA-based gene transfer with high transfection efficiency would be desirable. In this study, when US/MB was combined, naked HGF plasmid injected into the blood pool in the LV chamber, not the direct injection or intracoronary injection, was successfully transferred into the myocardium as evidenced by significant expression of HGF protein at day 7, which was related to the limited infarct size and subsequent LV remodeling. Although a relatively high dose of the plasmid could be

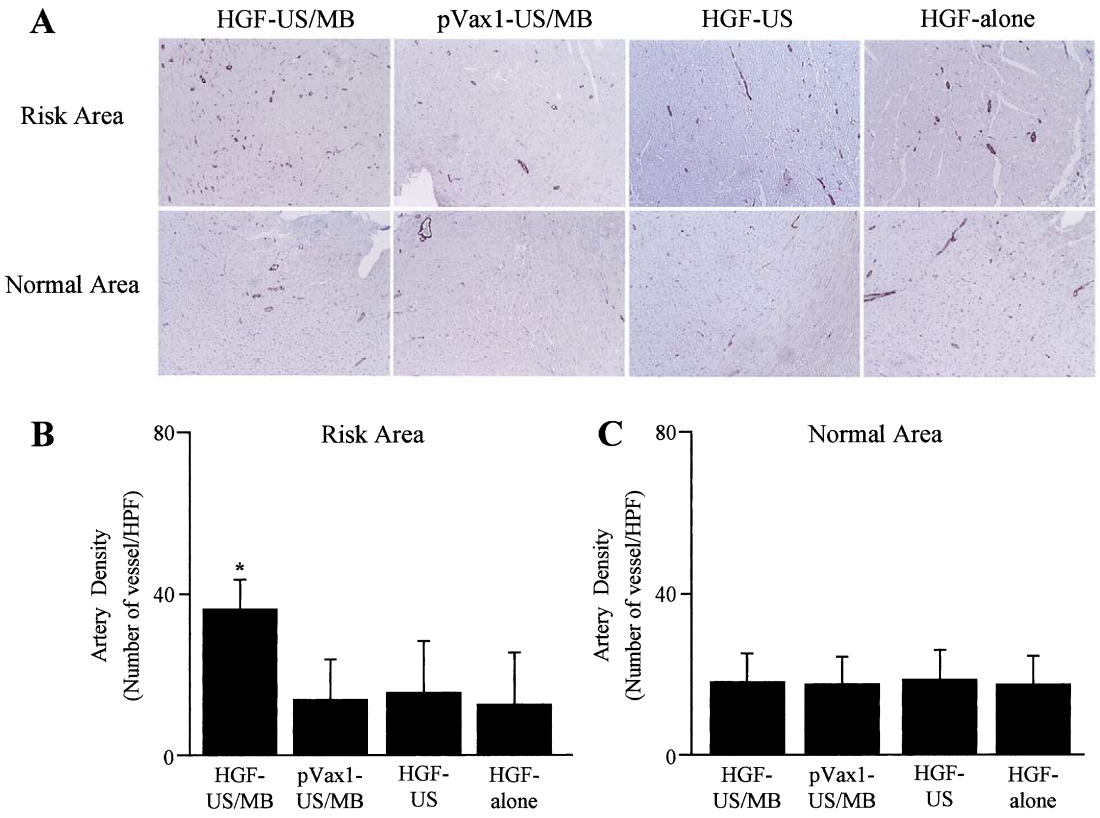

Figure 7. Anti-α-smooth muscle actin immuno-stain (×100 magnification). **(A)** In the regions adjacent to the scar, significant increase in arterial density was demonstrated only in a rat from HGF-US/MB but not in the other groups **(top)**. These groups showed similar vascular density in the remote non-infarcted regions **(bottom)**. **Bar graphs** compare the count of vessels per high-power field (HPF) among the groups for the regions adjacent to the infarction scar **(B)** and for the remote non-infarcted regions **(C)**. *$p < 0.05$ versus pVax1-US/MB, HGF-US, and HGF-alone. Abbreviations as in Figure 3.

needed for intravenous injection to achieve the similar plasmid concentration obtainable with intra-LV chamber injection, the present results provide the basis for the application of US/MB for non-viral transfection of therapeutic genes into the myocardium by systemic administration of the naked plasmid.

Insonation with such a low-frequency and high mechanical index as employed in this study may increase the permeability of endothelium even in the absence of MBs especially in application in rats offering less ultrasound attenuation, which may enhance the transfection of plasmids. However, no significant enhancement of the transfection was achieved in the HGF-US group in our rat model. In a previous study, similar insonation condition (frequency of 1.8 MHz, mechanical index of 1.6) induced only a limited microvascular rupture in the rabbit hearts suspended in a buffer solution in the absence of MBs (26). Therefore, a greater disruption may be needed in the naked plasmid transfection, and the combination of microbubble infusion and insonation seems to be necessary for the future application to humans in which a greater attenuation is expected. On the other hand, as assessed with HGF expression, transfection of HGF plasmid was enhanced by US/MB also in the remote control regions located in the LV posterior wall where ultrasound would possibly be attenuated. Therefore, bioeffects of US/MB were likely homogeneous in the entire short-axis cross-section of LV wall.

Because the coronary artery was completely ligated, no antegrade perfusion existed in the risk area. Influx of MBs and the plasmid in the risk area are assumed to have been provided by the collateral circulation or by the Thebesian veins directly from LV chamber (27).

No significant increase in ventricular premature beats was observed during US/MB, and mortality rate in HGF-US/MB was similar to those in the other groups. Moreover, the pVax1-US/MB did not show further deteriorations of myocardial function or larger infarct size compared with those in HGF-alone that did not undergo US/MB. Thus, adverse effects of US/MB were not observed in the present study. Similarly, mortality rate was not significantly different between the rats who received HGF plasmid and those who received pVax-1. Thus, no significant adverse effects of HGF plasmid injection such as abnormal immune stimulation, cytokine activation, or hemodynamic impairment were observed in the present study.

Cardioprotection by HGF in MI. Higher HGF concentration in the vein collecting the blood from the territory of infarct related artery was shown to result in less severe LV enlargement in patients with reperfused acute MI (28). However, it has remained unknown whether transfer of

HGF gene to the myocardium in the acute phase of MI may attenuate progression of LV dysfunction in the chronic phase. In the present study, serial echocardiographic observations revealed that LV remodeling was much less, and LV function rather progressively improved in the group of HGF-US/MB. Importantly, the scar corresponding to the core of infarction was significantly smaller in this group, which resulted in the preserved inotropic reserve for sympathetic stimulation by isoproterenol. The effects of HGF are dependent on its binding to the transmembrane receptor encoded by the proto-oncogene, c-Met. In MI, c-Met expression was increased in the periphery of the infarcted region (29), and the sensitivity to and the effects of HGF are enhanced in this region, resulting in less cell death (3,4) and more angiogenesis (6). Thus, although HGF expression was enhanced also in the remote control regions in HGF-US/MB, angiogenesis and arteriogenesis were significantly enhanced only in viable regions surrounding the infarct area where c-Met/HGF receptor is known to be up-regulated (29).

Besides angiogenesis, the cardiac HGF system also exerts cytoprotective effects against ischemic injury through its anti-oxidative (3) and anti-apoptotic (4) effects, which may also contribute to salvage of ischemic myocardium. Hepatocyte growth factor stimulates the degradation of extracellular matrix and inhibits its synthesis induced by angiotensin II (30). Administration of human recombinant HGF prevented and/or regressed fibrosis in the liver (31) and the lung (32). Human HGF complementary DNA transfection to the myocardium by means of hemoagglutinating virus of Japan-liposome prevented myocardial fibrosis in an animal model developing cardiomyopathy (33). Thus, HGF can modulate wound-healing processes and prevent scar formation.

Hepatocyte growth factor expression level relatively early after the gene transfer might be sufficient to exert direct preventive effects on cell death under severe ischemia and/or augment the residual vascular function including recruitment of latent collateral vessels to reduce the ischemia. In the subacute phase, angiogenesis became significant, which further improved myocardial ischemia, while anti-fibrotic action played a role in preventing scar formation. Decrease in infarct size can limit subsequent mechanical stress and neurohumoral stimulation to non-infarcted region resulting in increased LV mass. All these processes may be integrated into the successful prevention of postinfarction remodeling by HGF gene transfer to the heart at acute phase of MI.

In HGF-US/MB, we observed a 60% reduction in infarct size (scar size) compared with those in controls. This was relatively greater than those seen in previous reports on infarct-limiting effects of basic fibroblast growth factor by 45% (34) or with cerivastatin by 49% (35), both of which were evaluated in acute phase. Progressive expansion of infarct region occurred by three weeks after MI only in the ineffectively treated groups, while it was almost absent in the HGF-US/MB group in our study. This may be a reason for the greater relative reduction of scar size in our effective treatment group.

Study limitations. Because the capillaries identified by alkaline phosphatase stain sometimes formed a continuous network rather than punctate cross-sections in the margins of viable regions in the HGF-US/MB group, the angiogenesis quantitated as the capillary count in this study might be underestimated in these regions.

Because we infused the plasmid into the circulating blood pool, a relatively high dose of HGF plasmid (1,500 μg/body) was necessary compared with previous studies (20 μg/body [19] and 100 to 500 μg/body [11]) that employed the direct intra-tissue injection of the plasmid. To avoid possible alterations of acoustic properties of the MB that has been approved for clinical use in many countries, the plasmid was not loaded on the shell of MB as in previous studies (17,21). The naked plasmid injected into the blood is easily degraded by DNase or captured by non-specific scavenger receptors (36), which leads to rapid decrease in concentration of the plasmid reaching the target regions. Therefore, we chose to inject the plasmid into the LV chamber rather than the peripheral vein. Incorporation or attachment of the plasmid on the MB shell may overcome such limitations. This may enable the local release of plasmid at the region where US is applied and, thereby, would reduce the required dose of plasmid or would enable intravenous injection of the plasmid, which was not tested in this study.

The efficiency of gene transfection by US/MB should be dependent upon insonation conditions as well as MBs structure. Therefore, further studies are necessary to optimize the insonation condition in the specific target organs with various acoustic properties in larger animals. Similarly, because capillary disruption is known to occur in the settings of clinical MCE and presumably underlies the present results as the mechanism, future studies should pursue the tradeoff between the efficacy and safety in respect to MB concentration and US intensity.

Acknowledgments

The authors are grateful to AnGes MG Inc., Tokyo, Japan, for providing the naked plasmid encoding HGF.

Reprint requests and correspondence: Dr. Koji Ohmori, The Second Department of Internal Medicine, Kagawa University School of Medicine, 1750-1, Ikenobe, Miki-cho, Kita-gun, Kagawa 761-0793 Japan. E-mail: komori@kms.ac.jp.

REFERENCES

1. McKay RG, Pfeffer MA, Pasternak RC, et al. Left ventricular remodeling after myocardial infarction: a corollary to infarct expansion. Circulation 1986;74:693–702.
2. Matsumoto K, Nakamura T. Hepatocyte growth factor (HGF) as tissue organizer for organogenesis and regeneration. Biochem Biophys Res Commun 1997;239:639–44.
3. Ueda H, Nakamura T, Matsumoto K, Sawa Y, Matsuda H, Nakamura T. A potential cardioprotective role of hepatocyte growth factor in myocardial infarction in rats. Cardiovasc Res 2001;51:41–50.

4. Nakamura T, Mizuno S, Matsumoto K, Sawa Y, Matsuda H, Nakamura T. Myocardial protection from ischemia/reperfusion injury by endogenous and exogenous HGF. J Clin Invest 2000;106:1511–9.
5. Ueda H, Sawa Y, Matsumoto K, et al. Gene transfection of hepatocyte growth factor attenuates reperfusion injury in the heart. Ann Thorac Surg 1999;67:1726–31.
6. Aoki M, Morishita R, Taniyama Y, et al. Angiogenesis induced by hepatocyte growth factor in non-infarcted myocardium and infarcted myocardium: up-regulation of essential transcription factor for angiogenesis, etc. Gene Ther 2000;7:417–27.
7. Kass EA, Falck PE, Alvira M, et al. Quantitative determination of adenovirus-mediated gene delivery to rat cardiac myocytes in vitro and in vivo. Proc Natl Acad Sci USA 1993;90:11498–502.
8. French BA, Mazur W, Geske RS, et al. Direct in vivo gene transfer into porcine myocardium using replication-deficient adenoviral vectors. Circulation 1994;90:2414–24.
9. Verma IM, Somia N. Gene therapy: promises, problems and prospects. Nature 1997;389:239–42.
10. Tsurumi Y, Takeshita S, Chen D, et al. Direct intramuscular gene transfer of naked DNA encoding vascular endothelial growth factor augments collateral development and tissue perfusion. Circulation 1996;94:3281–90.
11. Taniyama Y, Morishita R, Aoki M, et al. Therapeutic angiogenesis induced by human hepatocyte growth factor gene in rat and rabbit hindlimb ischemia models: preclinical study for treatment of peripheral arterial disease. Gene Ther 2001;8:181–9.
12. Lin H, Parmacek MS, Morle G, et al. Expression of recombinant genes in myocardium in vivo after direct injection of DNA. Circulation 1990;82:2217–21.
13. Losordo DW, Vale PR, Symes JF, et al. Gene therapy for myocardial angiogenesis: initial clinical results with direct myocardial injection of phVEGF165 as sole therapy for myocardial ischemia. Circulation 1998;98:2800–4.
14. Vale PR, Losordo DW, Milliken CE, et al. Randomized, single-blind, placebo-controlled pilot study of catheter-based myocardial gene transfer for therapeutic angiogenesis using left ventricular electromechanical mapping in patients with chronic myocardial ischemia. Circulation 2001;103:2138–43.
15. Skyba DM, Price RJ, Linka AZ, Skalak TC, Kaul S. Direct in vivo visualization of intravascular destruction of microbubbles by ultrasound and its local effects on tissue. Circulation 1998;98:290–3.
16. Price RJ, Skyba DM, Kaul S, Skalak TC. Delivery of colloidal particles and red blood cells to tissue through microvessel ruptures created by targeted microbubble destruction with ultrasound. Circulation 1998; 98:1264–7.
17. Shohet RV, Chen S, Zhou YT, et al. Echocardiographic destruction of albumin microbubbles directs gene delivery to the myocardium. Circulation 2000;101:2554–6.
18. Lawrie A, Brisken AF, Francis SE, Cumberland DC, Crossman DC, Newman CM. Microbubble-enhanced ultrasound for vascular gene delivery. Gene Ther 2000;7:2023–7.
19. Taniyama Y, Tachibana K, Hiraoka K, et al. Development of safe and efficient novel nonviral gene transfer using ultrasound: enhancement of transfection efficiency of naked plasmid DNA in skeletal muscle. Gene Ther 2002;9:372–80.
20. Taniyama Y, Tachibana K, Hiraoka K, et al. Local delivery of plasmid DNA into rat carotid artery using ultrasound. Circulation 2002;105: 1233–9.
21. Teupe C, Richter S, Fisslthaler B, et al. Vascular gene transfer of phosphomimetic endothelial nitric oxide synthase (S1177D) using ultrasound-enhanced destruction of plasmid-loaded microbubbles improves vasoreactivity. Circulation 2002;105:1104–9.
22. Beeri R, Guerrero JL, Supple G, Sullivan S, Levine RA, Hajjar RJ. New efficient catheter-based system for myocardial gene delivery. Circulation 2002;106:1756–9.
23. Oshita A, Ohmori K, Yu Y, et al. Myocardial blood flow measurements in rats with simple pulsing contrast echocardiography. Ultrasound Med Biol 2002;28:459–66.
24. Kramer MS, Feinstein AR. Clinical biostatistics. LIV. The biostatistics of concordance. Clin Pharmacol Ther 1989;46:309.
25. Hughes GC, Lowe JE, Kypson AP, et al. Neovascularization after transmyocardial laser revascularization in a model of chronic ischemia. Ann Thorac Surg 1998;66:2029–36.
26. Ay T, Havaux X, Van Camp G, et al. Destruction of contrast microbubbles by ultrasound: effects on myocardial function, coronary perfusion pressure, and microvascular integrity. Circulation 2001;104:461–6.
27. Ansari A. Anatomy and clinical significance of ventricular Thebesian veins. Clin Anat 2001;14:102–10.
28. Yasuda S, Goto Y, Baba T, et al. Enhanced secretion of cardiac hepatocyte growth factor from an infarct region is associated with less severe ventricular enlargement and improved cardiac function. J Am Coll Cardiol 2000;36:115–21.
29. Sato T, Tani Y, Murao S, et al. Focal enhancement of expression of c-Met/hepatocyte growth factor receptor in the myocardium in human myocardial infarction. Cardiovasc Pathol 2001;10:235–40.
30. Taniyama Y, Morishita R, Nakagami H, et al. Potential contribution of a novel antifibrotic factor, hepatocyte growth factor, to prevention of myocardial fibrosis by angiotensin II blockade in cardiomyopathic hamsters. Circulation 2000;102:246–52.
31. Ueki T, Kaneda Y, Tsutsui H, et al. Hepatocyte growth factor gene therapy of liver cirrhosis in rats. Nat Med 1999;5:226–30.
32. Yaekashiwa M, Nakayama S, Ohnuma K, et al. Simultaneous or delayed administration of hepatocyte growth factor equally represses the fibrotic changes in murine lung injury induced by bleomycin: a morphologic study. Am J Respir Crit Care Med 1997;156:1937–44.
33. Taniyama Y, Morishita R, Aoki M, et al. Angiogenesis and antifibrotic action by hepatocyte growth factor in cardiomyopathy. Hypertension 2002;40:47–53.
34. Horrigan MC, Malycky JL, Ellis SG, et al. Reduction in myocardial infarct size by basic fibroblast growth factor following coronary occlusion in a canine model. Int J Cardiol 1999;68 Suppl 1:S85–91.
35. Wolfrum S, Grimm M, Heidbreder M, et al. Acute reduction of myocardial infarct size by a hydroxymetyl glutaryl coenzyme A reductase inhibitor is mediated by endothelial nitric oxide synthase. J Cardiovasc Pharmacol 2003;41:474–80.
36. Kawabata K, Takakura Y, Hashida M. The fate of plasmid DNA after intravenous injection in mice: involvement of scavenger receptors in its hepatic uptake. Pharm Res 1995;12:825–30.